Flow separation in the lee of bedforms: a numerical study on the influence of bedform height and length

Alice Lefebvre[1] Andries J. Paarlberg[2] and Christian Winter[3]

Abstract

This study investigates the flow separation zone that forms in the lee of steep bedforms. Flow velocities and water levels above bedforms are simulated using the numerical modeling system Delft3D. The simulated velocities are used to compute the position of the zero velocity points and flow separation line. The model was calibrated using lab velocity and water level measurements. It proved to correctly reproduce the size and shape of the flow separation zone as well as the water surface elevation. The model was then used to investigate the influence of bedform height and length on the flow separation in the lee of, and water level above, fixed alluvial bedforms. While a clear pattern of the influence of bedform height and length was recognized on the water levels, their impact on the length and shape of the flow separation zone was observed to be complex.

Key words: Bedforms, flow separation zone, numerical modeling

1. Introduction

Large asymmetric bedforms commonly develop in rivers. Over such bedforms, the pressure gradient at the edge of the bedform crest and over the steep lee side produces flow separation at the bedform crest and the formation of a recirculating eddy within the Flow Separation Zone (FSZ, Figure 1). From dimensional analysis, Engel (1981) suggested that the dimensionless length of the FSZ (length of FSZ / bedform height) was related to the ratio of bedform height and length (H_b / L_b), the ratio of depth and bedform height (h / H_b), grain roughness, and Froude number (u / $\sqrt{}$gh with u = velocity and g = acceleration due to gravity). He concluded from his laboratory experiments that the length of the flow separation is independent of the Froude number and flow depth but is dependent on the grain roughness for flat bedforms (H_b / L_b < 0.5) and decreases with increasing H_b / L_b. To the authors' knowledge, no systematic study of the influence of bedform height and length on the shape and length of the FSZ has been carried out since this classic work.

Large bedforms (dunes) affect the water surface by creating out-of-phase surface waves (Figure 1). These surface waves have been very little studied due to the inherent difficulties in measuring small water level variations created by bedforms and undisturbed by other phenomenons (e.g. wind). In particular, it is unknown whether the position of the lowest and highest points of the surface wave compared to the bedform crest and trough varies with bedform height and length.

The advance in numerical modeling allows numerical models to simulate flow fields and water levels above bedforms (e.g. El Kheiashy et al., 2010). Delft3D (Deltares, 2011) is an open-source flow and transport modeling system for the aquatic environment. It includes a non-hydrostatic module that has the potential to allow a precise simulation of flow over bedforms.

In this study we (1) calibrated and validated the Delft3D numerical model against lab data for the high-resolution simulation of flow over bedforms, with special interest in the FSZ and water levels and (2) determined the influence of the bedform height and length on the shape and length of the FSZ and characteristics of the water surface wave.

[1]MARUM- Center for Marine Environmental Sciences, University of Bremen, Leobener str, 28359 Bremen, Germany. alefebvre@marum.de
[2]HKV Consultants, P.O. Box 2120, 8203 AC Lelystad, the Netherlands. A.Paarlberg@hkv.nl
[3]MARUM- Center for Marine Environmental Sciences, University of Bremen, Leobener str, 28359 Bremen, Germany. cwinter@marum.de

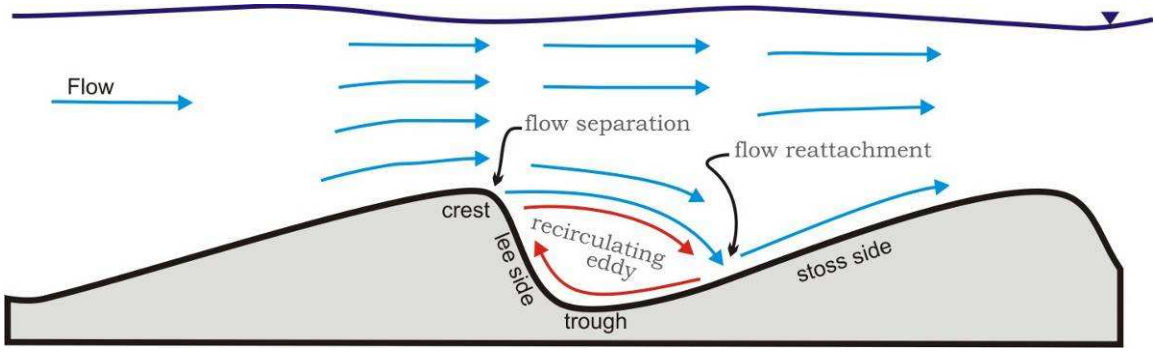

Figure 1. Flow separation zone in the lee of a bedform

2. Study methodology

We used the Delft3D numerical modeling system to simulate velocities and water level above bedforms. The simulated velocity profiles were used to evaluate the position of the flow separation points and to parameterize the flow separation line. The characteristics of the water surface wave were determined from the simulated water levels. In a first step, the model was validated against lab measurements of McLean et al. (1999). It was then used to perform systematically investigate the influence of bedform height and length on the FSZ.

2.1.*Numerical model*

In Delft3D-FLOW the 3D non-linear shallow water equations, derived from the three dimensional Navier-Stokes equations for incompressible free surface flow, are solved. In order to capture non-hydrostatic flow phenomena such as flow recirculation behind obstacles, the hydrostatic version of the Delft3D modeling suite is extended with a so-called weakly non-hydrostatic module. Using this module, the non-hydrostatic pressure is computed by using a pressure correction technique: for every time step, a hydrostatic step is first performed to obtain an estimate of the velocities and water levels; a second step, taking into account the effect of the non-hydrostatic pressure is then carried out and the velocities and water levels are corrected, such that continuity is fulfilled.

2.2.*Simulations set up*

All simulations were performed in a two-dimensional vertical (2DV) plane (Cartesian grid) over a fixed bed consisting of 20 bedforms. The boundary conditions were prescribed at the entrance as a constant depth-averaged velocity and at the exit as a constant water level of 0 m. The weakly non-hydrostatic version was used with the k-epsilon turbulence model. The bottom roughness was prescribed using the roughness length z_0 (z_0 = 0.0002 m for model validation at lab scale and z_0 = 0.01 m for model experiments at field scale). The grid size varied depending on the simulated bedform height in order to ensure an identical number of grid cells within the FSZ for all simulations.

2.3.*Flow separation zone*

The method to characterize the FSZ from the velocity profiles simulated by the numerical model was adapted from Paarlberg et al. (2007). The bedform considered was always the 16th out of the 20 simulated bedforms and the origin of the coordinate system was put at the crest horizontal position for x = 0 and at the trough vertical position for z = 0 (Figure 2). To enable comparison between the experiments, the longitudinal coordinate x and the vertical coordinate z were scaled with the bedform height (i.e. $x' = x / H_b$ and $z' = z / H_b$). For each velocity profile, the cells with negative horizontal velocity were identified and the height of the zero velocity point was determined (Figure 2). The height of the separation points was calculated along each profile by assessing the height at which the integral of the velocity between the bed

and that point was zero (see Paarlberg et al., 2007). The flow separation line s(x') was parameterized for each individual experiment by fitting a third-order polynomial function to the flow separation points:

$$s(x') = s_3 x'^3 + s_2 x'^2 + s_1 x' + s_0 \quad (1)$$

where $s_3 \ldots s_0$ are coefficients. In the experiments described in the present manuscript, the lee side was made of a single straight segment and therefore it was assumed that the separation point was at the bedform crest (Figure 2), giving $s_0 = 1$; moreover the flow separation line started with an angle of 0° compared to the horizontal, giving $s_1 = 0$. The intersection of the flow separation line with the bed defines the reattachment point. The flat bed intersection point was found from the intersection of the flow separation line and a horizontal bed whose elevation is that of the trough. The length of the flow separation zone ($L'_{st} = L_{st} / H_b$) was calculated as the horizontal distance between the crest and the flat bed intersection point and α_{rt} was defined as the angle of the flow separation line at the flat bed intersection point.

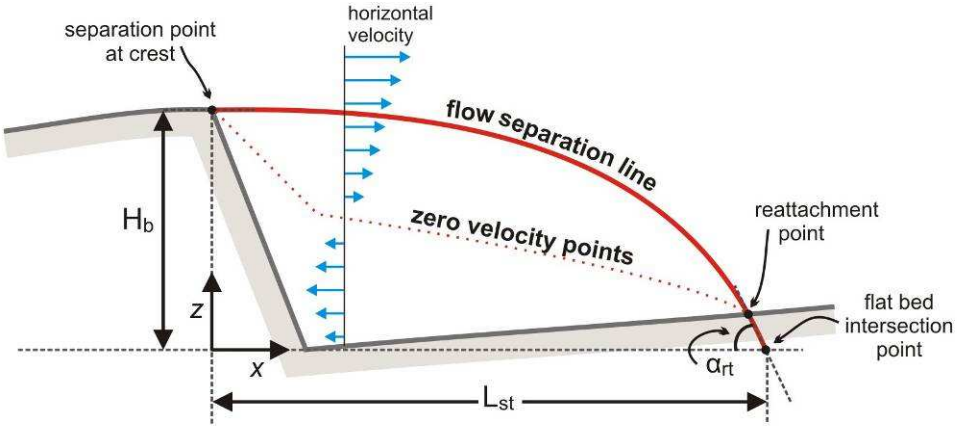

Figure 2. Schematic representation of flow separation in the lee of a bedform; H_b = bedform height; L_{st} = length of FSZ where the separation streamline would intersect a flat bed whose elevation is the same as the trough elevation and α_{rt} = angle of the flow separation line at the flat bed intersection point

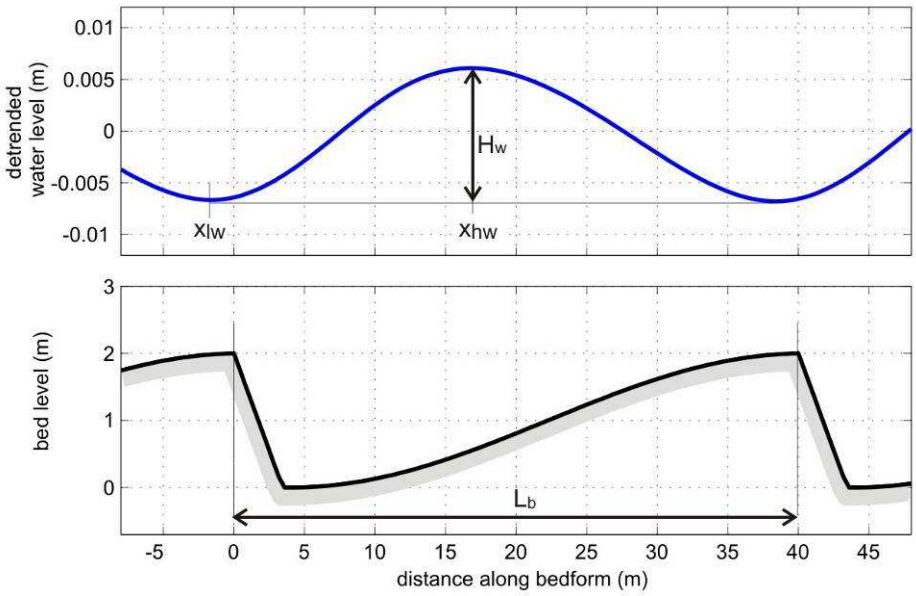

Figure 3: Definition of surface wave parameters; L_b = bedform length; H_w = surface wave height; x_{lw} = position of the lowest water level; and x_{hw} = position of the highest water level

The water surface characteristics were also determined for each simulation above the 16th bedform. The positions of the lowest and highest water levels (x_{lw} and x_{hw}) were calculated and the wave height H_w was determined as the height difference between those 2 points (Figure 3). To allow comparison, x_{lw} and x_{hw} are given normalized by H_b, $x'_{lw} = x_{lw} / H_b$ and $x'_{hw} = x_{hw} / H_b$.

3. Model validation

Six simulations were carried out in order to verify the model by inter-comparison with laboratory results from McLean et al. (1999) – referred to as ML - who carried out detailed measurements of velocity and water levels during 6 runs over bedforms 0.04 m high, 0.8 m or 0.4 m long and varying water depth and flow velocities (Table 1). In the original lab experiments, the flume bed was covered with 20 concrete bedforms having a straight lee side with a slope of 30° and a stoss side shape following a cosine curve. For each run, McLean et al. (1999) measured flow velocity and water level over the 16th bedform in order to characterize equilibrium conditions that were not perturbed by entrance and exit conditions.

Table 1. Water depth, flow velocity and dimensions of the bedforms used by McLean et al. (1999) for lab measurements of flow above bedforms. h = water depth; u = average velocity; Fr = Froude number; L_b = bedform length; H_b = bedform height

	h (m)	u (m s^{-1})	Fr	L_b (m)	H_b (m)	h / H_b	L_b / h	H_b / L_b
ML2	0.158	0.39	0.31	0.808	0.04	4.0	5.1	0.05
ML3	0.546	0.28	0.12	0.808	0.04	13.7	1.5	0.05
ML4	0.159	0.38	0.3	0.408	0.04	4.0	2.6	0.10
ML5	0.159	0.2	0.16	0.408	0.04	4.0	2.6	0.10
ML6	0.3	0.54	0.31	0.408	0.04	7.5	1.4	0.10
ML7	0.56	0.24	0.1	0.408	0.04	14.0	0.7	0.10

Figure 4 shows an example of results from model simulations and lab measurements illustrating that the model was able to simulate reverse flow within the flow separation zone. Comparison of the normalized length of the flow separation zone and the angle of the flow separation line at the flat bed intersection point calculated from McLean et al. (1999) lab measurements and model results were in good agreement (Figure 5). In particular, L'_{st} showed a difference of only 4% on average between values calculated from the model results and the lab measurements. The values of α_{rt} displayed more deviations between those values calculated from lab measurements and those calculated from model results. From the velocity profiles measured in the lab, the values of α_{rt} varied between -0.62° (ML7) and -0.39 (ML2) whereas α_{rt} calculated from the modeled velocities varied between -0.42° and -0.43° for runs ML3 to ML7 and had a value of -0.36° for ML2.

The difference in data resolution may explain the discrepancy observed in Figure 5, since the number of velocity points used to calculate the zero velocity and flow separation points greatly differ between the lab and model data (Figure 4). Results from the lab data were calculated from 15 to 32 velocity measurements situated within the flow separation zone whereas 306 to 410 velocity points were available to calculate the flow separation points from the model results. Because of the limited number of points available from the lab measurements, Paarlberg et al. (2007), following a suggestion from McLean, carried out a sophisticated extrapolation of the velocity profiles towards the bed. For those profiles where several velocity points were recognized, the velocity below the lowest available point was calculated using a log-linear extrapolation. The calculated velocity integral of the profiles containing at least two negative velocity points was then used to extrapolate negative velocity profiles that had only one negative velocity point using a log-linear-quadratic equation. The results of this extrapolation can be seen on Figure 4: the lab measurements are shown with stars and the extrapolation velocity data near the bed are visualized with the plain lines. This method gave extremely good results however it relies on a substantial assumption and handling of the data for determining the height of the flow separation points. The numerical model allows a better data resolution within the flow separation zone by simulating velocity points at a greater number of heights

above the bed than what was measured in the lab. Therefore the height of the flow separation points can be calculated based on much more data points and is more reliable.

Furthermore, the number of velocity profiles used to parameterize the flow separation line also differs, i.e. the horizontal resolution of the lab experiments was also scarcer than that of the model results. In this study, we re-analyzed Paarlberg et al. (2007) parameterization of McLean et al. (1999) data and calculated somewhat different values of L'_{st} and α_{rt} than in the original publication. That is mainly due to the fact that we decided to discard velocity profiles near the reattachment point that contained only one negative velocity point because they were considered to be unreliable, especially when the measured velocity was very little (< 0.01 m s^{-1}). The difference between L'_{st} calculated in the present study and by Paarlberg et al. (2007) are between 1 and 10% and do not show any specific trend, i.e. the model results compared to one or the other is no better or worse. However, this highlights the sensitivity of the results calculated from the lab measurements to data processing carried out to determine the position of the flow separation points.

Finally and probably more importantly, Paarlberg et al. (2007) used the reattachment point to parameterize the flow separation line since the small profiles did not allow a unique parameterization using only the velocity profiles with negative velocities. To calculate the position of the reattachment point, they assumed that the zero velocity line was a straight line and fitted a linear regression to the zero velocity points (Figure 4). However, the high number of velocity points available from the model results showed that the zero velocity line is not composed of a single straight segment. With the bedform morphology used by ML (straight lee side and cosine stoss side), the zero velocity was composed of two segments: a straight part between the crest and the trough (i.e. above the lee side) and a curved part between the trough and the reattachment point which was best parameterized using a 3rd order polynomial. Assuming a straight zero velocity line might have lead to wrongly estimate the position of reattachment point, which influenced the parameterization of the flow separation line and results in uncertainty on the values of L'_{st} and α_{rt} calculated from the lab measurements.

Considering the aspects regarding grid resolution and different methods to calculate the position of the reattachment point, the agreement between values of L'_{st} and α_{rt} calculated from lab measurements and model simulation is considered good and the model is thought to correctly capture the size and shape of the flow separation zone.

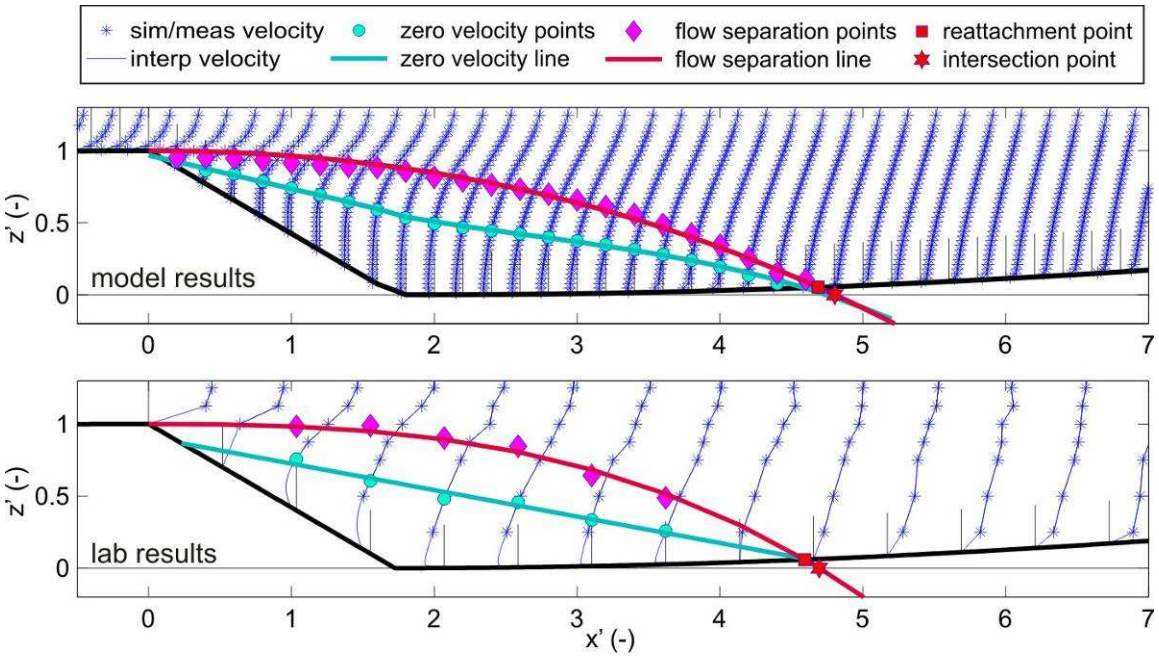

Figure 4. Illustration of velocity data (measured in the lab or simulated by the numerical model and interpolated between the measured/simulated points), zero velocity points and separation line from model results (top) and lab measurements (bottom) for run ML3

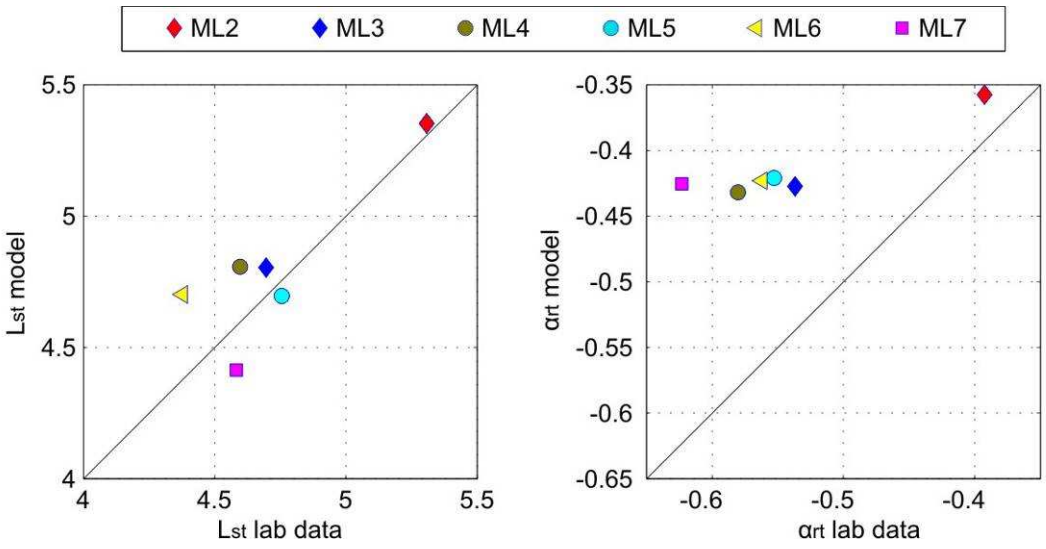

Figure 5. Comparison of results from lab data and model simulations

A good agreement was also observed between the water levels measured by McLean et al. (1999) and simulated with the numerical model (Figure 6). The comparison was particularly good for shallower simulations which produced a relatively large surface wave (e.g. H_w = 1 mm for ML4). It was less good for deeper simulations for which the variations of water levels were very small (e.g. H_w = 0.002 mm for ML7) and could not be captured precisely in the lab.

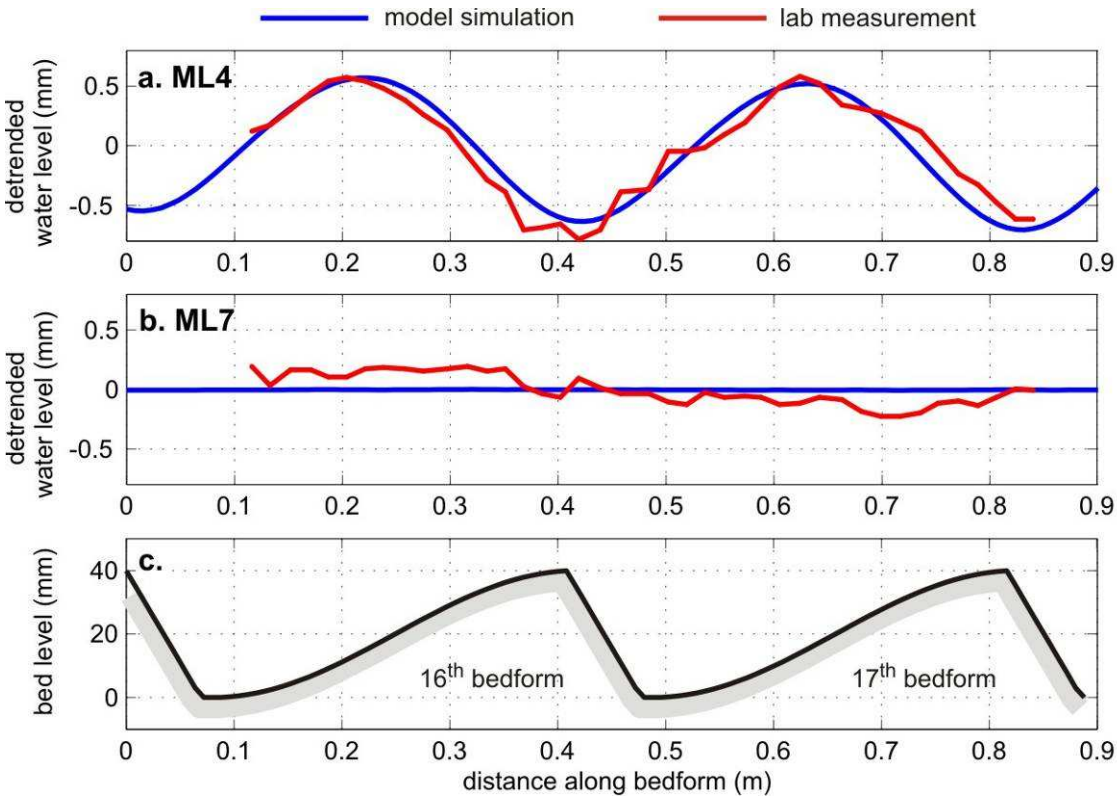

Figure 6. Simulated and measured water levels for runs (a) ML4 and (b) ML7 and (c) bed level for both runs

4. Model experiments

Three experiments were designed, each composed of 5 simulations (Table 2) to investigate the influence of bedform height and length on the shape and length of the FSZ. The flow properties and bedform dimensions in the experiments were chosen to resemble river conditions. Dune (i.e. bedforms that affect and are affected by the water surface) dimensions in rivers typically scale with flow depth (Venditti (in press) based on Allen (1982) dataset):

$$2.5 < h / H_b < 20; \text{ on average } h / H_b = 6 \quad (2)$$

$$1 < L_b / h < 16; \text{ on average } L_b / h = 5 \quad (3)$$

Furthermore, the ratio of bedform height to bedform length (H_b / L_b) for dunes is generally between 0.01 and 0.1 (Venditti, in press).

In all simulations the average water depth was 8 m and the depth-averaged velocity was 1 m s^{-1}. Bedforms dimensions were varied in accordance to Equations 2 and 3 and the resulting H_b / L_b is in the range of the typical H_b / L_b for dunes. In all simulations, the domain was composed of 20 bedforms having a stoss side that follows a cosine curve and a straight lee side with an angle equal to the angle of repose (30°). Bedforms simulated for experiment 1 had simultaneously varying height and length in order to assess the influence of bedforms dimensions on bedforms with a constant shape (Figure 7). Bedforms simulated for experiment 2 had a constant length (average length of experiment 1) and varying height (same variations as in experiment 1) and those for experiment 3 had a constant height (average height of experiment 1) and varying length (same variations as in experiment 1). For those two experiments, because the lee side angle was always 30°, changes in the bedform length or height resulted in variations of bedform shape (Figure 8 and 9), going from longer, flatter bedforms (low H_b / L_b) to shorter, steeper bedforms (high H_b / L_b). However, since the lee side was always 30°, the position of the trough itself was always at 1.73 H_b.

Table 2. Water depth, flow velocity and dimensions of the bedforms used for the experiments. h = water depth; u = average velocity; Fr = Froude number; L_b = bedform length; H_b = bedform height

h (m)	u (m s^{-1})	Fr	L_b (m)	H_b (m)	h / H_b	L_b / h	H_b / L_b
			Experiment 1				
			64.0	3.2	2.5	8.0	
			32.0	1.6	5.0	4.0	
8	1	0.113	21.4	1.1	7.5	2.7	0.05
			16.0	0.8	10.0	2.0	
			10.7	0.5	15.0	1.3	
			Experiment 2				
			64.0			8.0	0.02
			32.0			4.0	0.04
8	1	0.113	21.4	1.4	5.6	2.7	0.07
			16.0			2.0	0.09
			10.7			1.3	0.13
			Experiment 3				
				3.2	2.5		0.11
				1.6	5.0		0.06
8	1	0.113	28.8	1.1	7.5	5.0	0.04
				0.8	10.0		0.03
				0.5	15.0		0.02

4.1. *Simultaneously varying height and length (constant shape)*

When varying simultaneously the bedform height and length with constant water depth and flow velocity, the normalized length of the FSZ and the angle of the flow separation line at the flat bed intersection point were observed to increase with increasing bedform dimensions, L'_{st} varying from 4.5 to 5.7 and α_{rt} varying from -0.46 to -0.35 within the bedform dimensions tested (Figure 7). Overall, smaller bedforms were observed to generate a shorter and steeper FSZ than larger bedforms.

The height of the surface wave also increased with increasing bedform dimensions with wave height varying from 0.03 to 2.5 cm within the bedform dimensions tested. The position of lowest and highest water levels along the bedform were constant with x'_{lw} = -1 (i.e. the lowest water level was found 1 bedform height before the crest) and x'_{hw} = 8.7 (i.e. the highest water level was situated 7 bedform height after the trough).

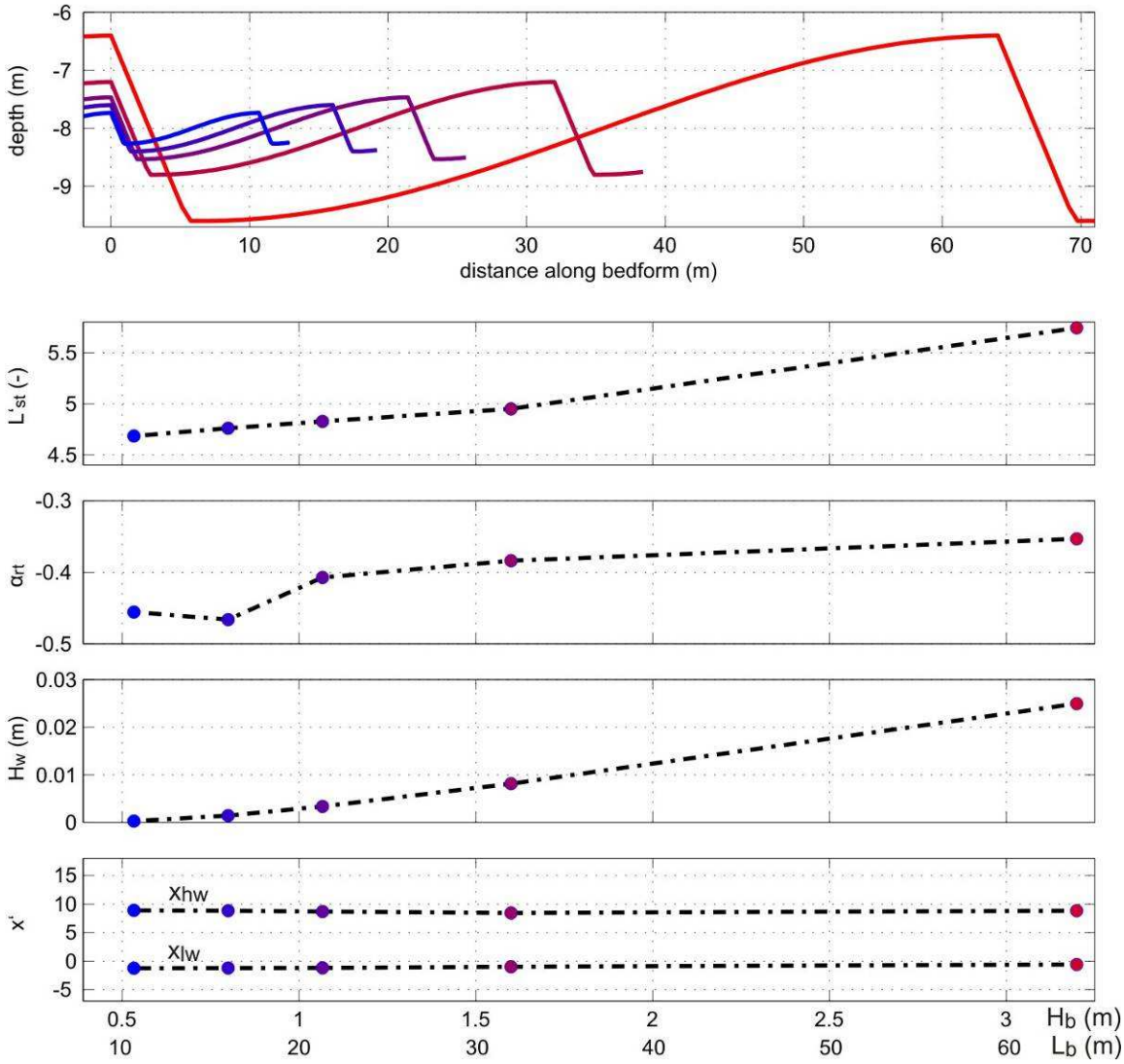

Figure 7. Results of experiment 1

4.2.*Varying length, constant height*

When varying the bedform length while keeping constant bedform height, water depth and flow velocity, longer (flatter) bedforms generated a longer and flatter FSZ than shorter (steeper) bedforms. The normalized length of the FSZ and the angle of the flow separation line at the flat bed intersection point were observed to increase with increasing bedform length, L'_{st} varying from 4.4 to 5.2 and α_{rt} varying from -0.49 to -0.37 within the bedform dimensions tested (Figure 8). The height of the surface wave also increased with increasing bedform length with wave height varying from 0.06 to 1.1 cm for bedform lengths between 10.7 and 64 m. As the bedform shape changed, the position of lowest and highest water levels along the bedform changed: for the shortest (steepest) bedform tested, the lowest water level was situated 0.6 H_b *after* the crest and the highest point at 4.4 H_b after the crest (2.7 H_b after the trough). For the longest (flattest) bedform tested, the lowest water level was situated at 2.8 H_b *before* the crest and the highest point at 13.7 H_b after the crest (12.0 H_b after the trough).

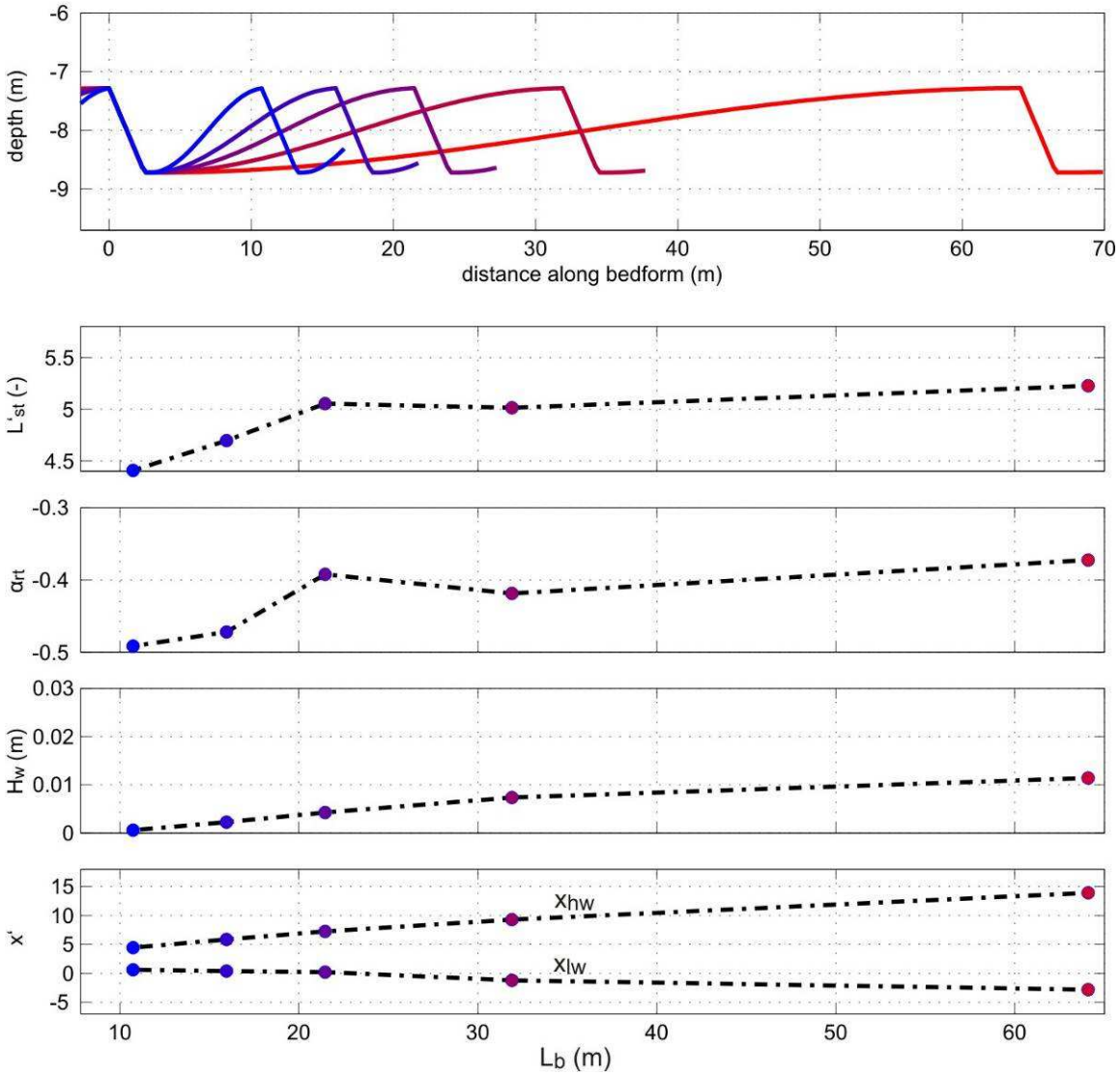

Figure 8. Results of experiment 2

4.3.*Varying height, constant length*

When varying the bedform height and keeping bedform length, water depth and flow velocity constant, the normalized length of the FSZ and the angle of the flow separation line at the flat bed intersection point slightly increased with increasing bedform height apart from the highest bedform tested over which were calculated values as low as for the smallest bedform. For heights ranging from 0.5 to 1.6 m, L'_{st} varied from 4.7 to 5.1 and α_{rt} varying from -0.41 to -0.38; for a bedform height of 3.2 m however, L'_{st} = 4.7 and α_{rt} = -0.42 (Figure 9). Therefore, higher (steeper) bedforms generated a longer steeper flow separation zone than smaller (flatter) bedforms, apart from the highest bedform tested.

The height of the surface wave increased with increasing bedform height with H_w varying from 0.3 to 1.3 cm within the bedform heights tested. Similarly to experiment 2, as the bedform shape changed, the position of lowest and highest water levels along the bedform changed: for the highest (steepest) bedform tested, the lowest water level was situated at 0.4 H_b *after* the crest and the highest level at 5.2 H_b after the crest (3.5 H_b after the trough). For the lowest (flattest) bedform, the lowest water level was situated at 6.8 H_b before the crest and the highest point at 17.4 H_b after the crest (15.7 H_b after the trough).

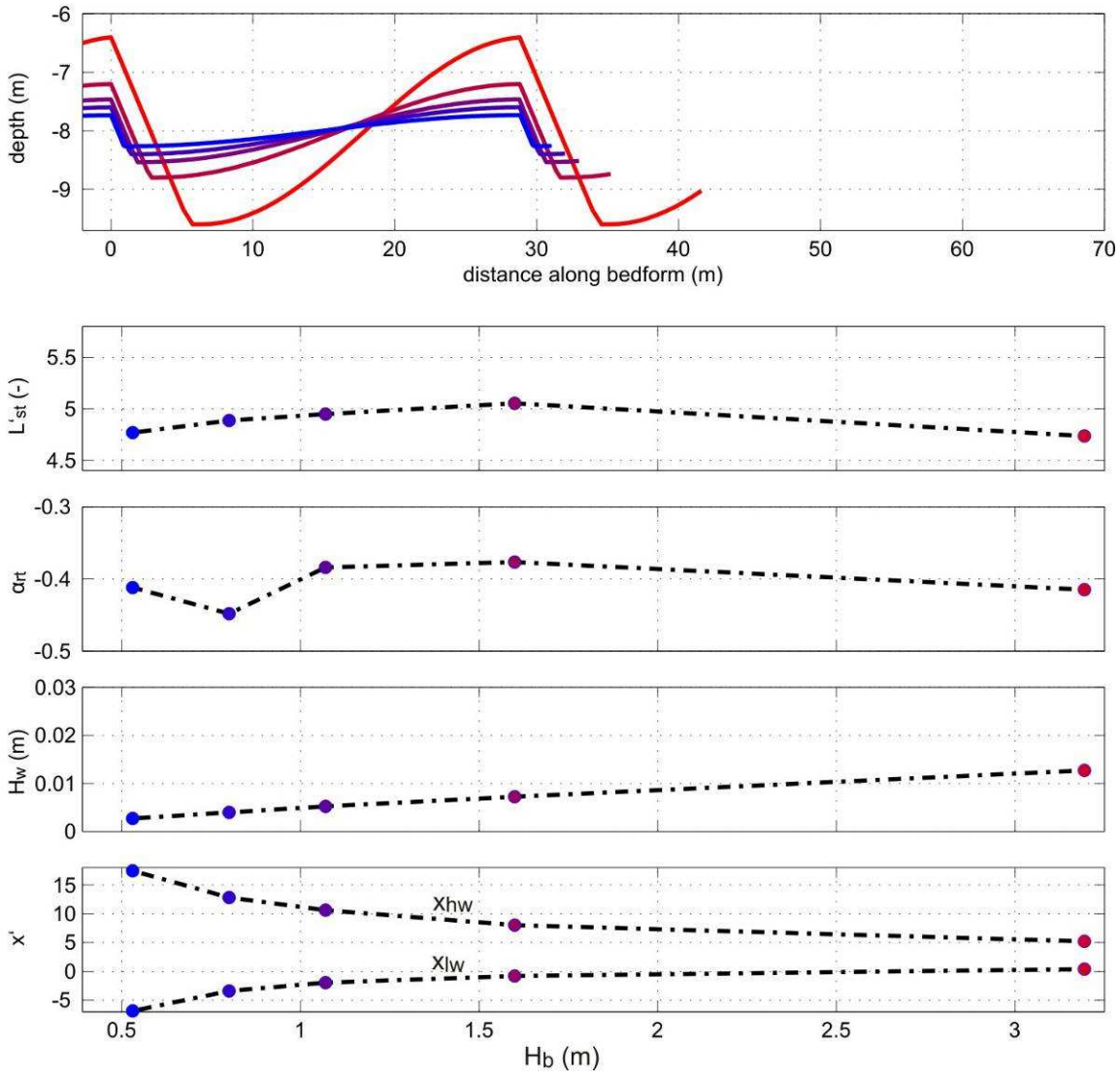

Figure 9. Results of experiment 3

4.4.*Synthesis*

Considering the three experiments collectively (Figure 10), L'_{st}, α_{rt} and H_w calculated when varying both height and length simultaneously or only one parameters were relatively similar except for the highest and longest bedform tested. Both bedform height and length had an influence on the shape and length of the FSZ and varying bedform height and/or bedform length resulted in variation of L'_{st} and α_{rt}. There was no clear relationship between H_b / L_b and L'_{st} or α_{rt}. Although results from experiments 2 and 3 were similar for H_b / L_b around 0.05, they differed for higher and lower H_b / L_b.

Both bedform height and length displayed a positive relationship with H_w, which increased as height and/or length increased. As a result H_w calculated from experiments 2 and 3 displayed opposite trends when plotted as a function of H_b / L_b.

The positions of the lowest and highest water levels above the bedform were solely related to the bedform shape and did not vary for bedforms with constant shape. The value of x'_{lw} increased with increasing H_b / L_b. The lowest water level was situated before the bedform crest for flatter bedforms (low H_b / L_b) and after the crest for H_b / L_b > 0.05. The value of x'_{hw} decreased with increasing H_b / L_b. The highest water level was always situated after the bedform trough.

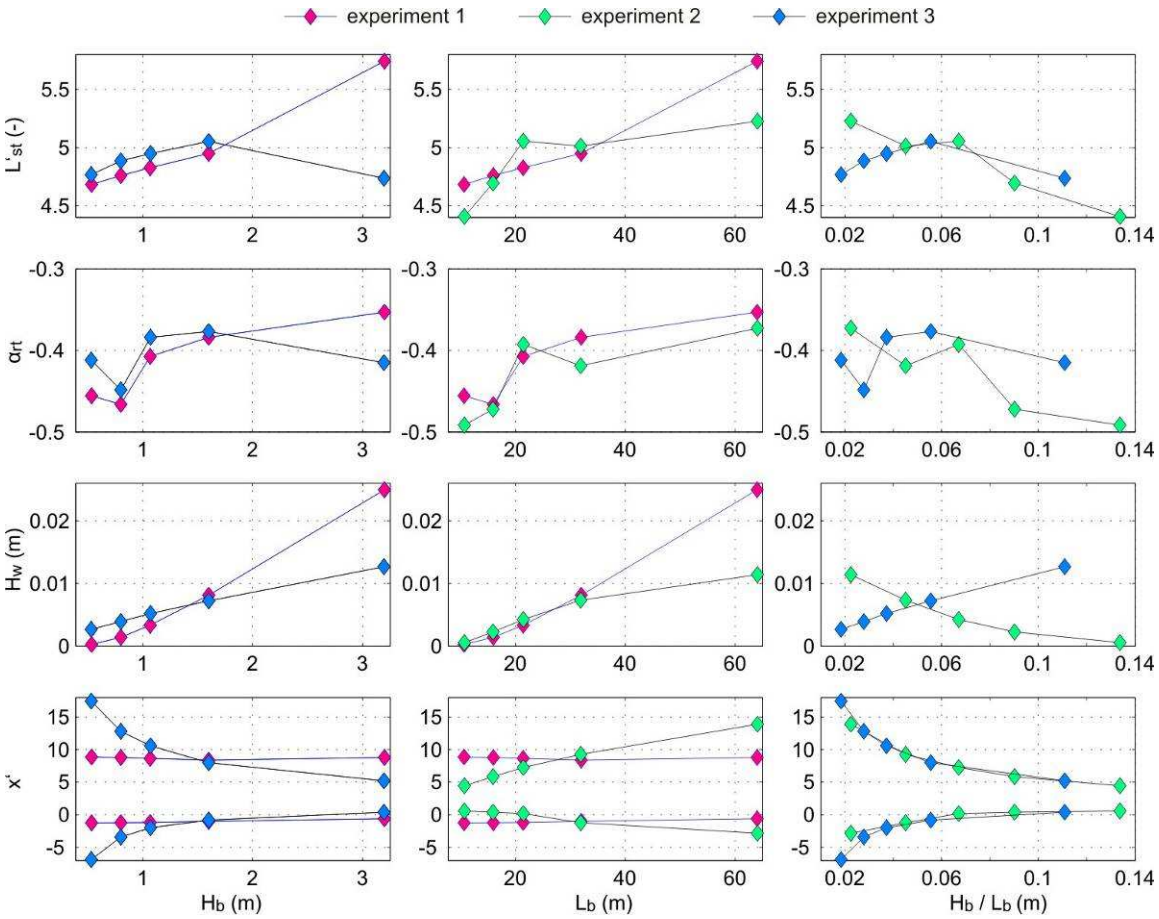

Figure 10. Synthesis of results from the 3 experiments

5. Discussion and conclusions

Delft3D numerical model used with the weakly non-hydrostatic module was shown to correctly reproduce the length and shape of the flow separation zone on the lee of bedforms if compared to the classical Mclean et al (1999) dataset. The high data resolution that can be achieved using the numerical model revealed the shape of the zero velocity line, composed of a straight segment over the straight lee side and a curved

segment over the lower stoss side investigated in the present study. It seems logical that the shape of the zero velocity line is related to the shape of the bed and agrees with zero velocity points inferred from other studies (e.g. Buckles et al., 1984, Ruck and Makiola, 1993). The bedforms studied here were made of relative simple shapes. It is currently unknown what the shape of the zero velocity line over natural bedforms having more complicated shape (e.g. having several brink points over the lee side) is and it can be wondered whether it would consist of several segments.

The three model experiments carried out allowed to test the influence of some of the parameters suggested to control the length of the flow separation zone by Engel (1981). The grain roughness and Froude number were kept constant so we could not assess their influence on the FSZ and we concentrated this study on testing the influence of bedform height and length. Engel (1981) concluded that h / H_b did not influence the normalized length of the flow separation zone for Froude numbers smaller than 0.5. Our results suggest the contrary as already argued by Puls (1983) on the discussion of Engel (1981) work. The combined influence of bedform height and length of the flow separation zone was observed to be complex and no clear trend appeared relating the normalized length of the flow separation zone and H_b / L_b. The results obtained by changing the bedform length showed an overall decrease of the normalized length of the FSZ, as observed by Engel (1981) when also varying bedform length. However changing the bedform height produced different results for bedforms with a similar shape suggesting that both H_b / L_b and h / H_b simultaneously influence the length and shape of the flow separation zone. The influence of water depth therefore also needs to be determined.

The numerical model proved to correctly simulate water level variations above bedforms. The experiments showed that the height of the water level wave was affected by variations in bedform height and length but was not related to H_b / L_b. On the contrary, the positions of the points of lowest and highest water levels were strongly related to bedform shape through the parameter H_b / L_b. In particular the point of lowest water level was situated before the crest for $H_b / L_b < 0.05$ and after the crest for $H_b / L_b > 0.05$. The point of higher water level was always situated after the trough.

Acknowledgements

The authors are grateful to Prof. Stephen McLean for sharing his data. This study was funded through DFG-Research Center / Cluster of Excellence “The Ocean in the Earth System”. Alice Lefebvre acknowledges the support of GLOMAR – Bremen International Graduate School for Marine Sciences.

References

Allen, J. R. L., 1982. *Sedimentary Structures: Their Character and Physical Basis*, Elsevier.

Buckles, J., Hanratty, T. J. and Adrian, R. J., 1984. Turbulent flow over large-amplitude wavy surfaces. *Journal of Fluid Mechanics*, 140: 27-44.

Deltares, 2011. *User Manual Delft3D-FLOW*, Deltares.

El Kheiashy, K., McCorquodale, J., Georgiou, I. and Meselhe, E., 2010. Three dimensional hydrodynamic modeling over bed forms in open channels. *International Journal of Sedimentary Research*, 25 (4): 431-440.

Engel, P., 1981. Length of Flow Separation over Dunes. *Journal of the Hydraulics Division*, 107 (10): 1133-1143.

McLean, S. R., Wolfe, S. R. and Nelson, J. M., 1999. Spatially averaged flow over a wavy boundary revisited. *Journal of Geophysical Research*, 104 (C7): 15743-15753.

Paarlberg, A. J., Dohmen-Janssen, C. M., Hulscher, S. J. M. H. and Termes, P., 2007. A parameterization of flow separation over subaqueous dunes. *Water Resources Research*, 43: W12417.

Ruck, B. and Makiola, B., 1993. The Flow over the Inclined Step. *Notes on Numerical Fluid Mechanics*, 40: 47-55.

Venditti, J. G., in press. *Bedforms in sand-bedded rivers*, Academic Press.

Puls, W., 1983. Discussion of "Length of Flow Separation over Dunes". *Journal of Hydraulic Engineering*, 109(1): 139-140.